

Symmetry-dependent electronic Raman scattering in $\text{La}_{2-x}\text{Sr}_x\text{CuO}_4$: Evidence for doping-induced change in the k -space anisotropy of charge dynamics

T. Katsufuji and Y. Tokura

Department of Physics, University of Tokyo, Tokyo 113, Japan

T. Ido* and S. Uchida

Superconductor Research Course, University of Tokyo, Tokyo 113, Japan

(Received 22 July 1993)

Low-frequency electronic Raman scattering in $\text{La}_{2-x}\text{Sr}_x\text{CuO}_4$ has been investigated over a wide compositional region, $0 \leq x \leq 0.34$, covering the insulating, superconducting, and non-superconducting metallic compounds. We have found that the scattering intensity for the (xy) polarization predominates over that of the $(x'y')$ polarization in the low-doping region below $x \leq 0.15$, but vice versa at higher doping levels. The results indicate that anisotropy in the effective-mass tensor (or k -space dispersion) of the carriers changes systematically with hole doping, in contradiction with the simple band picture.

Doping-induced change in the charge dynamics of CuO_2 -layered compounds has been of considerable interest in light of the mechanism of high- T_c superconductivity as well as the more general problem of the Mott transition. The purpose of this paper is to present, by Raman spectroscopy, experimental evidence which indicates a doping-induced anomalous change in the k -space charge dynamics in $\text{La}_{2-x}\text{Sr}_x\text{CuO}_4$.

As one of the unconventional features of normal state properties in cuprate superconductors, electronic Raman scattering has been under extensive experimental as well as theoretical investigations.¹ In most of the high- T_c cuprate compounds with optimized T_c a nearly temperature- (T -) independent flat spectrum has been observed over a wide range of the scattering frequency (at least up to $\sim 5000 \text{ cm}^{-1}$) above T_c . The feature is quite in contrast with the conventional electronic Raman scattering spectrum observed in a doped semiconductor which shows a one-particle excitation continuum with a cutoff frequency $\omega = qv_F$ and a peak in the plasma frequency region with a vanishing intensity near $\omega \sim 0$.

Concerning this problem, Cardona² has proposed an interpretation in terms of the neutral carrier density fluctuation model,³⁻⁵ which was originally devised to explain the electronic Raman scattering spectra and their polarization dependence in heavily doped Si. In those compounds, the effective-mass tensors around the Fermi surfaces are locally anisotropic and these carriers cause "neutral carrier density fluctuation" without Coulombic screening, which can produce a strong scattering intensity. This model can account for the specific selection rule or the polarization dependence of the scattering intensity in heavily doped n -Si (Ref. 3) and p -Si.⁴ Moreover, their spectral shape can be well reproduced by postulating the relaxational function $\omega\Gamma/(\omega^2 + \Gamma^2)$. In fact, the same functional form has been used for analysis of the electronic Raman spectra in layered cuprate compounds⁶ assuming that the inverse relaxation time Γ is a function of both temperature (T) and frequency (ω). The nearly ω - and T -independent spectrum as observed in high- T_c

cuprates could be explained by a strongly ω - and T -dependent Γ in a specific manner which should reflect the unconventional feature of the quasiparticle dynamics near the Fermi level.

In this paper, we report on the electronic Raman scattering spectra of $\text{La}_{2-x}\text{Sr}_x\text{CuO}_4$ over a wide compositional region, $0 \leq x \leq 0.34$. In particular, we will focus on a doping-induced change of the polarization (symmetry) dependence of the depolarized scattering intensity, which has enabled us to investigate a change in anisotropy of the effective-mass tensor of the charge carriers.

Single crystals of $\text{La}_{2-x}\text{Sr}_x\text{CuO}_4$ used in the present study were the same specimens as used in previous optical studies,⁷ and details of the sample preparation and characterization were all described in Ref. 7. The samples with $x = 0.10, 0.15$, and 0.20 show superconducting transitions at $T_c = 18, 27$, and 22 K , respectively, while the *overdoped* samples with $x = 0.26$ and $x = 0.34$ show metallic but not superconducting behavior. The directions of the crystallographic axes were determined by Laue back reflection and all the samples were mechanically polished with $0.3 \mu\text{m}$ alumina. For measurements of polarized Raman spectra, a 514.5-nm light beam from an argon ion laser (30 mW) was focused into a 0.1-mm -diam spot and the nearly backward scattered light was collected and dispersed by a triple monochromator equipped with an intensified-diode-array detector. The spectral resolution was set to 15 cm^{-1} in this experiment. The Raman spectra were measured for the two depolarized geometries $(x'y') = (x+y, x-y)$ and (xy) . The notation x (or y) represents the polarization of the incident or scattered light along the in-plane Cu-O-Cu direction. In the tetragonal setting for the crystal structure, the scattering geometries $(x'y')$ and (xy) correspond to the symmetries B_{1g} and B_{2g} , respectively. The spectral intensities were calibrated to the instrumental sensitivity as well as the penetration depth of the incident and scattered light which was derived from optical conductivity data of the same crystals.⁷ The temperature of the sam-

ple was estimated by measuring the ratio of the intensity of the Stokes and anti-Stokes shifts. Raman scattering measurements were also made by using a 488.0-nm line as an incident light, but no difference was observed within experimental accuracy as far as the intensity ratio of the $(x'y')$ to (xy) spectrum was concerned.

We show in Fig. 1 the Raman spectra below 600 cm^{-1} for the $(x'y')$ and (xy) polarizations at 100 K with varying the doping level x . The inset shows an overall feature up to 5000 cm^{-1} for the undoped ($x = 0$) crystal. A broad and intense peak around 3000 cm^{-1} for the $(x'y')$ polarization can be ascribed to the two-magnon excitation.⁸ Prominent peak structures in the region of $200\text{--}1500\text{ cm}^{-1}$ for the $x = 0$ spectra correspond to one-phonon or two-phonon scattering⁹ which perhaps arises from the leakage of A_{1g} modes. Apart from those phonon peaks, however, the spectra of the undoped sample ($x = 0$) bear little intensity in the low-frequency region below 600 cm^{-1} for both symmetries.

When holes are introduced by Sr doping, the scattering intensity for the (xy) polarization is notably enhanced as seen in the $x = 0.06$ spectrum and dominates over that for the $(x'y')$ polarization at low doping levels. As x increases further, the scattering intensity for the $(x'y')$ polarization tends to increase and finally predominates over that for the (xy) polarization in the overdoped region. Incidentally, in the case of $\text{YBa}_2\text{Cu}_3\text{O}_{7-\delta}$ with T_c of 90 K,¹⁰ their flat Raman spectra and symmetry dependence in the normal state resembles those observed in the high-doped region ($x > 0.2$) of $\text{La}_{2-x}\text{Sr}_x\text{CuO}_4$ crystals.

The intensity of electronic Raman scattering is related to the imaginary part of the response function of the electronic system such as

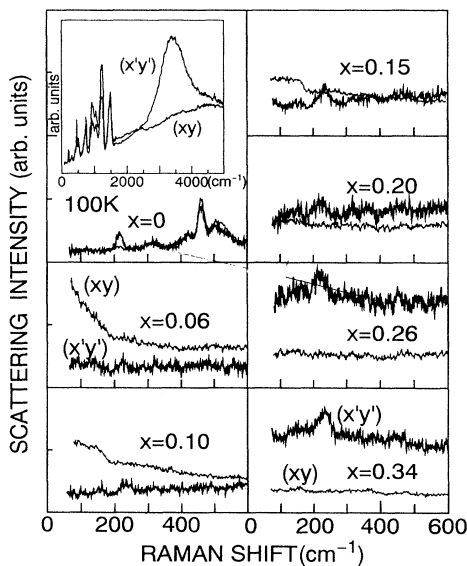


FIG. 1. Raman spectra in $\text{La}_{2-x}\text{Sr}_x\text{CuO}_4$ for the $(x'y')$ and (xy) polarization at 100 K below 600 cm^{-1} . The scale for the scattering intensity is common for all the spectra, which are calibrated to the instrumental sensitivity as well as the penetration depth of the incident and scattered light. The inset shows the $x = 0$ spectra up to 5000 cm^{-1} at 100 K.

$$I(\omega) = [1 + n(\omega)]\chi''(\omega), \quad (1)$$

where $n(\omega) = [\exp(\hbar\omega/k_B T) - 1]^{-1}$ is the Bose factor. Figure 2 shows the polarization- and T -dependent $\chi''(\omega)$ derived from the observed spectra (Fig. 1) by the above equation. At $x = 0.10$, $\chi''(\omega)$ for the $(x'y')$ polarization is nearly T independent, but $\chi''(\omega)$ for the (xy) polarization varies with temperature. Such a T -dependent feature of $\chi''(\omega)$ in the $x = 0.10$ sample for the (xy) polarization is similar to that of $\text{YBa}_2\text{Cu}_3\text{O}_{7-\delta}$ for the $(x'y')$ polarization. In fact, the $x = 0.10$ Raman spectra for the (xy) polarization can be well reproduced by assuming a T - and ω -dependent relaxation time, as in the case of $\text{YBa}_2\text{Cu}_3\text{O}_{7-\delta}$.⁸ Dashed lines in the $x = 0.10$ (xy) spectra indicate the result of the curve fitting by the functional form of

$$\chi''(\omega) = B\omega\Gamma/(\omega^2 + \Gamma^2). \quad (2)$$

Here, B is a constant [see also Eq. (4)] and inverse of the relaxation time (Γ) was assumed to be in the form of⁶

$$\Gamma = \sqrt{(\alpha\omega)^2 + [\Gamma_0(T)]^2}, \quad (3)$$

where the *marginal Fermi liquid* model¹¹ requires the T -linear scattering rate $\Gamma_0(T) = \beta T$. The best-fit parameters for the $x = 0.10$ (xy) spectrum are $\alpha = 0.32$, $\Gamma_0(T = 100\text{ K}) = 110\text{ cm}^{-1}$ and $\Gamma_0(T = 300\text{ K}) = 330\text{ cm}^{-1}$ (i.e., $\beta = 1.1\text{ cm}^{-1}/\text{K}$). Thus the obtained reasonable fitting guarantees that the low-lying continuum for the (xy) spectrum of the $x = 0.10$ sample is due to electronic excitations. By contrast, the rather T -independent $\chi''(\omega)$ for the $(x'y')$ polarization at $x = 0.10$ can hardly arise from excitations of the carriers, but is likely to be the low-energy tail of the higher-lying excitations, perhaps the damped two-magnon excitations.¹²

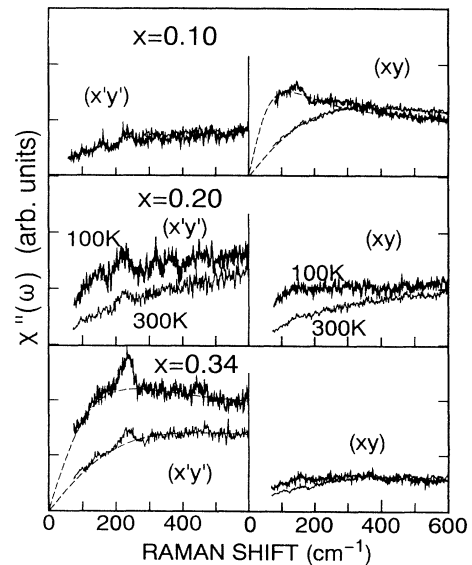


FIG. 2. Polarization and temperature dependence of the imaginary part of the response function $[\chi''(\omega)]$. The scale for χ'' is common for all the spectra. Dashed lines are the fitted curves by Eqs. (2) and (3) in the text. For the values of the fitting parameters, see the text.

In the $x = 0.20$ crystal, $\chi''(\omega)$ is T dependent for both polarizations and the spectral weight is comparable to each other, as seen in Fig. 2. This signals that the electronic Raman scattering process contributes to the low-frequency spectra for both polarizations at this doping level. Finally, in the heavily doped ($x = 0.34$) crystal, $\chi''(\omega)$ for the $(x'y')$ polarization remains T dependent and its spectral weight becomes much larger than that for the (xy) polarization. An appropriate set of parameters [$\alpha = 0.45$, Γ_0 ($T = 100$ K)=220 cm^{-1} , and Γ_0 ($T = 300$ K)=380 cm^{-1}] can reproduce the experimental data as shown by the dashed lines in Fig. 2, although $\Gamma_0(T)$ rather deviates from the T -linear relation (as also observed in the case of $\text{YBa}_2\text{Cu}_3\text{O}_{7-\delta}$ crystals⁶). The obtained parameter values α and $\Gamma_0(T)$ are comparable with those for $\text{YBa}_2\text{Cu}_3\text{O}_{7-\delta}$ system.⁶ These results ensure that the T -dependent low-frequency $\chi''(\omega)$ spectra in metallic $\text{La}_{2-x}\text{Sr}_x\text{CuO}_4$ are of an electronic origin relevant to the carrier dynamics, in spite of the anomalous symmetry and doping dependence of their intensity.

To extract at most the low-lying electronic contribution and at least the higher-lying magnetic one, we take the intensity ratio (R) of the $(x'y')$ to (xy) spectrum at 100 cm^{-1} , the lowest frequency in the present experiment. Figure 3 shows the result of R as a function of x . R increases continuously with x from 0.26 for $x = 0.06$ to 3.15 for $x = 0.34$ at 100 K. A larger R value was observed at 300 K in the low- x region than at 100 K, though a similar crossover behavior was observed. Such an apparent temperature dependence of R is likely due to the tail component of the high-energy excitation spectra, which is not negligible in particular for the $(x'y')$ polarization at low doping levels and at higher temperature (300 K). In this context, the R values measured at 100 K reflect better the genuine process of electronic Raman scattering.

In order to interpret the observed doping-induced

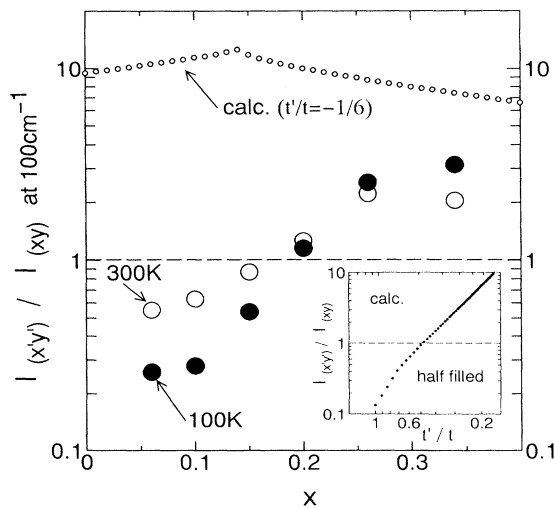


FIG. 3. The ratio of the Raman scattering intensity for the $(x'y')$ polarization to that for the (xy) polarization at 100 cm^{-1} . The small circles show the calculated ratio by the band model (see text). The inset displays the calculated ratio with changing t'/t in the tight-binding model.

change in the symmetry dependence of the scattering intensity, we adopt here the aforementioned neutral carrier density fluctuation model.^{2,5} In this model, the scattering intensity is given such as in Eqs. (1) and (2). The prefactor B in Eq. (2), which determines the scattering intensity as well as its symmetry dependence, is given by the relation,²

$$B = \frac{\hbar e^4}{\pi c^4} \frac{dN}{dE_F} \left\langle \left[\mathbf{e}_L \cdot \left(\frac{1}{\overleftrightarrow{m}} - \left\langle \frac{1}{\overleftrightarrow{m}} \right\rangle \right) \cdot \mathbf{e}_S \right]^2 \right\rangle, \quad (4)$$

where \mathbf{e}_S and \mathbf{e}_L are the polarization vectors of incident and scattered light, \overleftrightarrow{m} is the effective-mass tensor, and $\langle \dots \rangle$ represents the average over the Fermi surface. This model was originally based on the one-electron band scheme and the well-defined Fermi surface. We assume that the relation approximately holds even in the strongly correlated electron system as far as the effective-mass tensor of the charge carriers can be well defined.

The band calculation for the high- T_c cuprate compounds shows that the Fermi surface extends to the [100] direction,¹³ as schematically shown in Fig. 4(a). The anisotropic feature of the Fermi surface by an elaborate band calculation is essentially unchanged against the doping levels (i.e., the band filling),¹³ which should always result in the predominant $(x'y')$ scattering intensity over the (xy) one because of the mass anisotropy with respect to the [100] direction. An appropriate set of transfer integrals t (nearest neighbor) and t' (next-nearest neighbor) can be chosen¹⁴ to reproduce the Fermi surface structure in the $\text{La}_{2-x}\text{Sr}_x\text{CuO}_4$ system. We have applied the neutral carrier density fluctuation model to the calculation of R with changing the doping levels x , by using the parameter set ($t'/t = -1/6$) which reproduces the Fermi surface of the band calculation. The result is shown in Fig. 3, which gives $R = 7$ –12 over the whole x region. Such a simple prediction is consistent (at least qualitatively) with the experimental result for the overdoped compounds ($x > 0.20$) where the band calculation is believed to work well. However, the observed feature in the low-doping region that the intensity for the (xy) polarization is appreciably larger than that for the $(x'y')$ polarization cannot be explained by the band model.

The possible structure of the Fermi surface, which can give rise to a stronger scattering intensity for the (xy) polarization, is illustrated in Figs. 4(b) and 4(c). The hole pocket structure at $k = (\pm\pi/2, \pm\pi/2)$ depicted in Fig. 4(b) has been conjectured for a lightly hole-doped correlated insulator.^{15,16} These Fermi surfaces, or rigorously what we should call *energy contour lines* in the k -space dispersion of the charge carriers, show a large anisotropy of the mass tensor with respect to the [110] direction. These situations are to be realized when the next-nearest neighbor transfer integral (t') is comparable to or even more dominant than the nearest neighbor transfer integral (t). At the low-doping levels where the antiferromagnetic correlation is strong, the carrier motion between the nearest site causes spin frustration, and hence the next-nearest neighbor transfer would be favored. The present observation implies a crossover behavior of the carrier dispersion from the feature depicted in Fig. 4(b) or 4(c) to the one in Fig. 4(a) with an in-

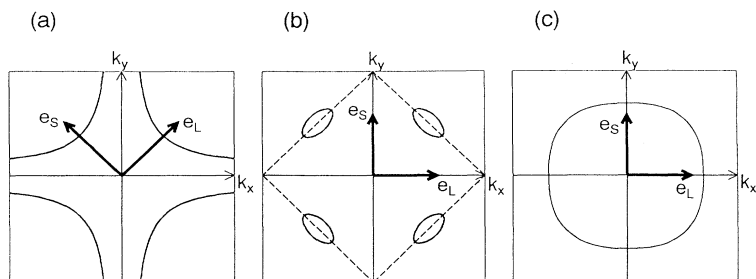


FIG. 4. Possible types of "Fermi surface" in $\text{La}_{2-x}\text{Sr}_x\text{CuO}_4$.

crease of x . For a test of this idea, the calculated results for R at half-filling with changing t'/t ratio are shown in the inset of Fig. 3. (The small deviation from half-filling does not cause appreciable change in R values.) The experimentally observed R , that is, from 0.26 ($x = 0.06$) to 3.15 ($x = 0.34$), is to be compared with the calculated result by changing t'/t from 0.8 to 0.28. [The Fermi surface in the case of $t'/t=0.8$ is similar to that shown in Fig. 4(c).]

Recent numerical calculations for the t - J model¹⁷ have proved the quasiparticlelike behavior of the single-particle Green's function even in the presence of a strong correlation, whose dispersion is similar to that of the non-interacting system. The above two scenarios [Fig. 4(b) or 4(c)] are apparently in contradiction with such a numerical result, as far as we assume that the calculated single-particle spectral function represents the anisotropy

of the effective-mass tensor. It is worth noting that a similar inconsistency between the observed charge dynamics and the predicted "Fermi surface" has also shown up in the interpretation of the anomalously x -dependent Hall coefficient ($R_H \sim +1/x$) in the low-doped region of the present system.¹⁸ Likewise, the present results obviously reflect an anomalous change of the anisotropic carrier dynamics caused by hole doping and hence can be an acid test for the theories which aim at understanding the normal state properties in cuprate compounds as a function of the doping level.

We are grateful to enlightening discussion with N. Nagaosa, H. Fukuyama, and M. Imada. The present work was supported by a Grant-In-Aid from the Ministry of Science, Education and Culture, Japan.

* Present address: Central Research Laboratories, Hitachi, Ltd. Kokubunji, Tokyo 185, Japan.

¹ For a review, see C. Thomsen, in *Light Scattering in Solids VI*, edited by M. Cardona and G. Güntherodt (Springer, Berlin, 1991), p. 321, and references therein.

² M. Cardona, *Physica C* **185-189**, 65 (1991).

³ M. Chandrasekhar, M. Cardona, and E. O. Kane, *Phys. Rev. B* **16**, 3579 (1977).

⁴ M. Chandrasekhar, U. Rössler, and M. Cardona, *Phys. Rev. B* **22**, 761 (1980).

⁵ I. P. Ipatova, A. V. Subashiev, and V. A. Voitenko, *Solid State Commun.* **37**, 893 (1981).

⁶ F. Slakey, M. V. Klein, J. P. Rice, and D. M. Ginsberg, *Phys. Rev. B* **43**, 3764 (1991).

⁷ S. Uchida, T. Ido, H. Takagi, T. Arima, Y. Tokura, and S. Tajima, *Phys. Rev. B* **43**, 7942 (1991).

⁸ K. B. Lyons, P. A. Fleury, J. P. Remeika, and T. J. Negran, *Phys. Rev. B* **37**, 2353 (1988).

⁹ S. Sugai, *Phys. Rev. B* **39**, 4306 (1989).

¹⁰ S. L. Cooper, F. Slakey, M. V. Klein, J. P. Rice, E. D. Bukowski, and D. M. Ginsberg, *Phys. Rev. B* **38**, 11934 (1988).

¹¹ C. M. Varma, P. B. Littlewood, S. Schmitt-Rink, E. Abrahams, and A. Ruckenstein, *Phys. Rev. Lett.* **63**, 1996 (1989).

¹² S. Sugai, S. Shamoto, and M. Sato, *Phys. Rev. B* **38**, 6436 (1988).

¹³ J. H. Xu, T. J. Watson-Yang, J. Yu, and A. J. Freeman, *Phys. Lett. A* **120**, 489 (1987).

¹⁴ T. Tanamoto, H. Kohno, and H. Fukuyama, *J. Phys. Soc. Jpn.* **61**, 1886 (1992).

¹⁵ B. Shraiman and E. D. Siggia, *Phys. Rev. Lett.* **60**, 740 (1988).

¹⁶ S. A. Trugman, *Phys. Rev. Lett.* **65**, 500 (1990).

¹⁷ W. Stephan and P. Horsch, *Phys. Rev. Lett.* **66**, 2258 (1991).

¹⁸ H. Takagi, T. Ido, S. Ishibashi, M. Uota, S. Uchida, and Y. Tokura, *Phys. Rev. B* **40**, 2254 (1989).